Metal-mediated base pairing within the simplified nucleic acid GNA†

Mark K. Schlegel, Lilu Zhang, Nicholas Pagano and Eric Meggers*

Received 17th September 2008, Accepted 24th October 2008
First published as an Advance Article on the web 1st December 2008
DOI: 10.1039/b816142a

Hydroxypyridone and pyridopurine homo- and hetero-base pairs have been investigated in the context of duplex GNA (glycol nucleic acid). Phosphoramidites for automated GNA solid phase synthesis were synthesized economically in a few steps starting from commercially available enantiopure glycidol. Similar to their behavior in DNA, the hydroxypyridone and pyridopurine homo-base pairs display a metal-dependent base pairing, with the hydroxypyridone base pair exhibiting a preference for copper(II) ions and the pyridopurine a preference for nickel(II) ions. However, these metallo-base pairs show modulated properties in GNA with respect to metal-dependent pairing stabilities and metal selectivities. Most interestingly, the hydroxypyridone homo-base pair and hydroxypyridone-pyridopurine hetero-base pair are particularly well accommodated in the GNA duplex and form copper(II)-dependent base pairs that are more stable compared to a Watson-Crick A:T base pair at the same position by nearly 20 °C and 24 °C, respectively. The structure of the copper(II)-hydroxypyridone homo-base pair is discussed based on a recent metallo-GNA duplex crystal structure.

Introduction

Due to its programmable self assembly, DNA is a promising biomaterial for the construction of nanoscale architectures (structural DNA nanotechnology) and has already been used for the assembly of a variety of periodic arrays in two dimensions and the construction of materials with predictable three-dimensional structures such as polyhedra and catenanes.[1] In this respect, an important current goal is the functionalization of DNA in order to create nanoscale devices with novel properties.[2] One recently developed strategy is the incorporation of metal-mediated base pairs into DNA, which enables one to place metal ions within the nucleobase π-stacking thus providing an Å-scale control of the patterning of metal ions along a helix axis.[3–6] It can easily be envisioned that a one dimensional array of redox-active metal ions, positioned along a DNA double helix by metal-mediated base pairing, may lead to nucleic acids with interesting magnetic and electronic properties. However, despite such exciting prospects for metal-mediated base pairing, the multistep synthesis of such artificial nucleotides, including the chromatographical separation of anomeric mixtures, is often painstaking and thus makes their future large scale utilization in nanoscale devices questionable.

Aware of this general problem, we recently developed the simplified nucleic acid GNA (glycol nucleic acid) which contains an acyclic backbone with propylene glycol nucleosides that are connected by phosphodiester bonds (Fig. 1).[7–10] Due to its unique combination of high duplex stability, high base pairing fidelity, and easy synthetic access of its nucleotide building blocks, GNA comprises an interesting scaffold for future nucleic acid nanotechnology. Current efforts in our laboratory therefore concentrate on introducing additional functionality into GNA, such as redox-active metal ions. As a first step into this direction, we recently reported the X-ray crystal structure of a GNA duplex containing two copper(II)-mediated base pairs.[8] Here we present the synthesis, incorporation, and pairing properties of three different metal-mediated base pairs in the context of GNA and discuss the structure of a GNA duplex containing two copper(II)-hydroxypyridone homo-base pairs.

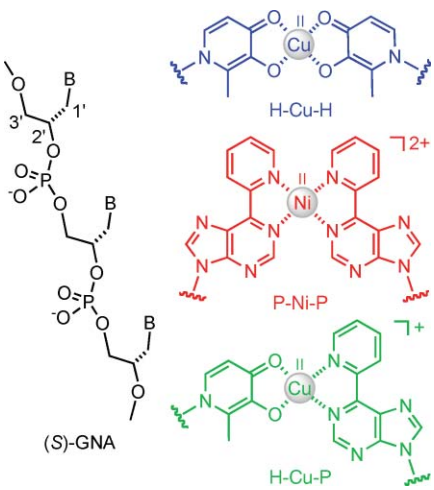

Fig. 1 Constitution of the (*S*)-GNA backbone and the metallo-base pairs investigated in this study.

Results and discussion

Synthesis of chelating nucleotides and incorporation into GNA

For our initial studies on metal-mediated base pairing in GNA, we chose a copper(II)-mediated hydroxypyridone homo-base pair (H–Cu–H, Fig. 1) and a nickel(II)-mediated pyridopurine homo-base pair (P–Ni–P, Fig. 1) scheme, both previously developed

Fachbereich Chemie, Philipps-Universität Marburg, Hans-Meerwein-Strasse, 35043 Marburg, Germany. E-mail: meggers@chemie.uni-marburg.de; Fax: (+49) 6421 2821534; Tel: (+49) 6421 2822189

† Electronic supplementary information (ESI) available: ^{1}H NMR spectra of compounds; GNA oligonucleotide synthesis and purification details. See DOI: 10.1039/b816142a

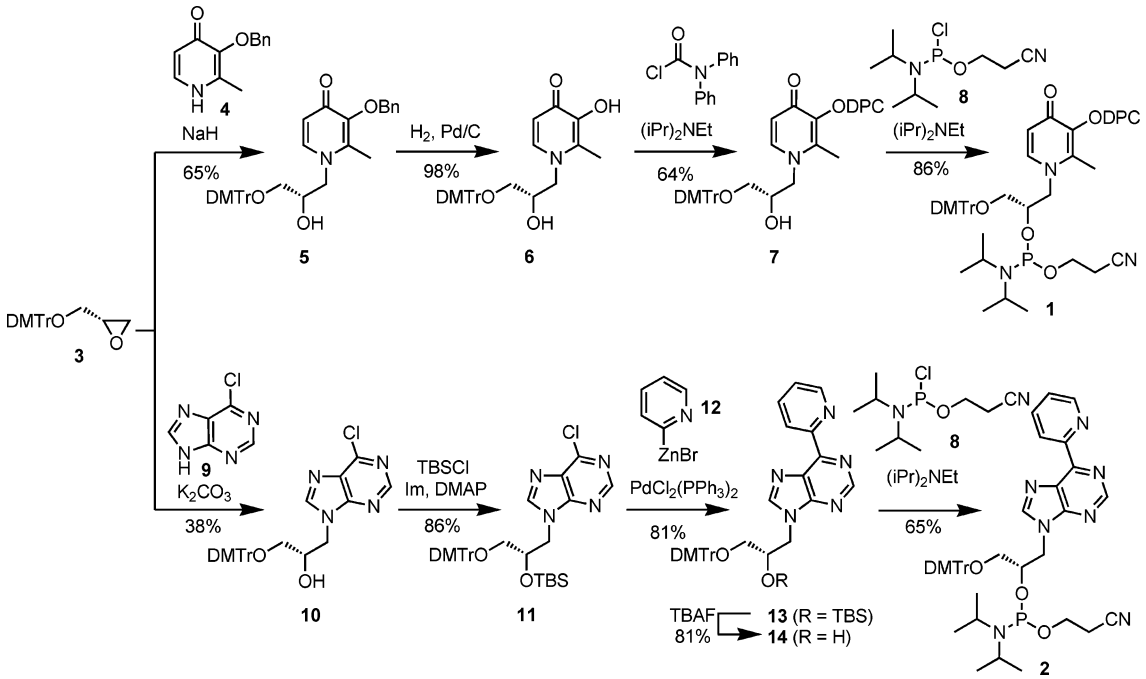

Scheme 1 Synthesis of phosphoramidites **1** and **2** for solid phase GNA oligonucleotide synthesis. DPC = diphenylcarbamoyl, DMTr = dimethoxytrityl.

for metal-mediated base pairing in DNA by Shionoya *et al.* and Switzer *et al.*, respectively.[4,5] Accordingly, we developed synthetic routes to the phosphoramidites **1** and **2** (Scheme 1). Phosphoramidite **1**, leading to hydroxypyridone homo-base pairs, was synthesized by the reaction of (*S*)-dimethoxytritylglycidol **3** with nucleobase **4** in the presence of catalytic amounts of NaH (0.22 equiv.) to afford **5** in a regioselective and stereospecific fashion in 65% yield. The benzyl protection group was subsequently removed by catalytic hydrogenation (**5**→**6**, 98%), followed by reprotection with a diphenylcarbamoyl (DPC) group to provide compound **7** in 64%. Finally, the GNA nucleoside **7** was converted into the phosphoramidite **1** by reacting with 2-cyanoethyl-*N*,*N*-diisopropylchlorophosphoramidite (**8**) in the presence of Hünig's base (86%). Overall, phosphoramidite **1** was synthesized from commercially available (*R*)-(+)-glycidol in 5 steps in an overall yield of 34%. This is a significant improvement over the corresponding 2′-deoxynucleotide for which a 9 step synthesis (including one additional step for the separation of an anomeric mixture) with an overall yield of 8.0% was reported starting from 2-methyl-3-benzyloxypyridone (**4**).[4,11]

Phosphoramidite **2** was synthesized in an analogous fashion by reacting (*S*)-dimethoxytritylglycidol **3** with 6-chloropurine (**9**) in the presence of K_2CO_3 (0.14 equiv.) to afford nucleoside **10** in 38% yield. After protection of the 2′-OH group with a *tert*-butyldimethylsilyl (TBS) group (**10**→**11**, 86%), the heterocycle of **11** was converted to the pyridopurine **13** by a Negishi coupling with 2-pyridylzincbromide **12** and $PdCl_2(PPh_3)_3$ (81%). Finally, after TBAF deprotection to **14** (81%), the phosphoramidite **2** was formed in 65% by the reaction with 2-cyanoethyl-*N*,*N*-diisopropylchlorophosphoramidite (**8**) in the presence of Hünig's base. Overall, this phosphoramidite **2** was synthesized starting from (*R*)-(+)-glycidol in 5 steps with an overall yield of 17% compared to the analogous 2′-deoxynucleotide for which starting with 2′-deoxy-D-ribose a 6 step synthesis with an overall yield of 26% was reported.[5,12,13]

With the phosphoramidites **1** and **2** in hand, the chelating hydroxpyridone (H) and pyridopurine (P) phosphoramidites were incorporated into GNA oligonucleotides by automated solid phase oligonucleotide synthesis using standard protocols for 2-cyanoethyl phosphoramidites. GNA oligonucleotides were synthesized in trityl-on mode, cleaved from the resin with concentrated ammonia at 55 °C overnight, purified by C18 reverse phase HPLC, detritylated with 80% acetic acid, and subsequently purified once again using a Waters XTerra column.

Metal-dependent duplex formation

In order to investigate the influence of metal ions on the thermal stabilities of the homo-base pairs H:H and P:P in GNA, the chelating nucleotides were introduced into the middle of a 15mer duplex (Table 1) and the melting temperatures (T_M) were determined by UV-monitored thermal melting. After removal of transition metal traces in the oligonucleotide solutions by treatment with the chelating resin Chelex 100 (Sigma), the pyridopurine base pair P:P leads to a marked destabilization of the GNA duplex by 15.5 °C compared to an A:T base pair at the same position (Table 1, entries 1 and 5). However, the addition of two equivalents of $NiCl_2$ strongly stabilizes the duplex, with an increase in the T_M value of 17.9 °C (Fig. 2 and Table 1, entry 6). Thus, with a T_M of 52.9 °C, the nickel(II)-containing P:P base pair is 2.4 °C more stable compared to an A:T Watson-Crick base pair at the same position (Table 1, entries 1 and 6). In contrast, metal salts such as $Pd(NO_3)_2$, $AuCl_3$, $ZnCl_2$, and $CdSO_4$ have no notable stabilization effect (Table 1, entries 10–13), whereas $Co(NO_3)_2$ (+7.0 °C), $CuCl_2$ (+ 7.3 °C), and $AgNO_3$ (+12.5 °C) stabilize the P:P base pair significantly (Table 1, entries 7–9).

Table 1 Thermal stabilities of GNA duplexes in the presence of metal ions[a]

3′-AATATTA**X**TATTTTA-2′
2′-TTATAAT**Y**ATAAAAT-3′

Entries	X:Y	Metal ions	T_M (°C)	ΔT_M (°C)[b]
1	A:T	none	50.5	
2	A:T	$NiCl_2$	51.0	+0.5
3	A:T	$CuSO_4$	50.8	+0.3
4	A:T	$ZnCl_2$	50.8	+0.3
5	P:P	none	35.0	
6	P:P	**$NiCl_2$**	**52.9**	**+17.9**
7	P:P	$AgNO_3$	47.5	+12.5
8	P:P	$CuCl_2$	42.3	+7.3
9	P:P	$Co(NO_3)_2$	42.0	+7.0
10	P:P	$CdSO_4$	36.5	+1.5
11	P:P	$ZnCl_2$	36.0	+1.0
12	P:P	$AuCl_3$	34.6	–0.4
13	P:P	$Pd(NO_3)_2$	32.8	–2.2
14	H:H	none	37.0	
15	H:H	**$CuSO_4$**	**70.2**	**+33.2**
16	H:H	$ZnCl_2$	52.9	+15.9
17	H:H	$Co(NO_3)_2$	42.1	+5.1
18	H:H	$Ni(NO_3)_2$	38.5	+1.5
19	H:H	$Cd(NO_3)_2$	37.9	+0.9
20	H:H	$AuCl_3$	37.1	+0.1
21	H:H	$AgNO_3$	37.0	0
22	H:H	$Pd(NO_3)_2$	36.6	–0.4
23	H:P	none	37.3	
24	H:P	**$CuSO_4$**	**74.4**	**+37.1**
25	H:P	$ZnCl_2$	50.9	+13.6
26	H:P	$Ni(NO_3)_2$	50.1	+12.8
27	H:P	$Co(NO_3)_2$	46.2	+8.9
28	H:P	$CdSO_4$	38.3	+1.0
29	H:P	$AuCl_3$	37.4	+0.1
30	H:P	$AgNO_3$	37.0	–0.3
31	H:P	$Pd(NO_3)_2$	36.4	–0.9

[a] Measurements performed in 10 mM sodium phosphate buffer, 100 mM $NaNO_3$, pH = 7.0. Each sample contained 2 μM of each strand and 4 μM of the specified metal salt. Data were measured at least in duplicate and the average taken. [b] Effect of the transition metal ion additives on the T_M values.

The nickel(II)-induced stabilization of the pyridopurine base pair in GNA is comparable with the stabilization of this base pair in the context of a DNA duplex (ΔT_M = +17.6 and 18.1 °C after the addition of two equivalents of $NiCl_2$ and $Ni(NO_3)_2$, respectively) reported by Switzer *et al*.[5] Similarly, in DNA $CoCl_2$ leads to a stabilization of the P:P base pair by +10.3 °C, whereas $AgNO_3$ and $CuCl_2$, in contrast to what is seen in GNA, do not provide significant stabilizations (ΔT_M = +2.0 and +2.9 °C, respectively). Thus, the pyridopurine base pair displays a modulated metal ion selectivity within the GNA duplex with a preference order of $Ni^{2+} > Ag^+ > Cu^{2+} \approx Co^{2+}$, compared to $Ni^{2+} > Co^{2+} >> Cu^{2+} \approx Ag^+$ in DNA.[5]

Whereas the pyridopurine base pair displays a preference for nickel(II) ions, the hydroxypyridone base pair is stabilized the strongest with copper(II) ions. In the absence of transition metal ions, the hydroxypyridone base pair H:H is destabilized in the context of the GNA duplex by 13.5 °C compared to an A:T base pair at the same position (Table 1, entries 1 and 14). The addition of two equivalents of $CuSO_4$ results in a strong increase in the T_M value by 33.2 °C (Fig. 2 and Table 1, entry 15). With a T_M of 70.2 °C, the copper(II)-containing H:H base pair is 19.7 °C more stable compared to an A:T Watson-Crick base pair

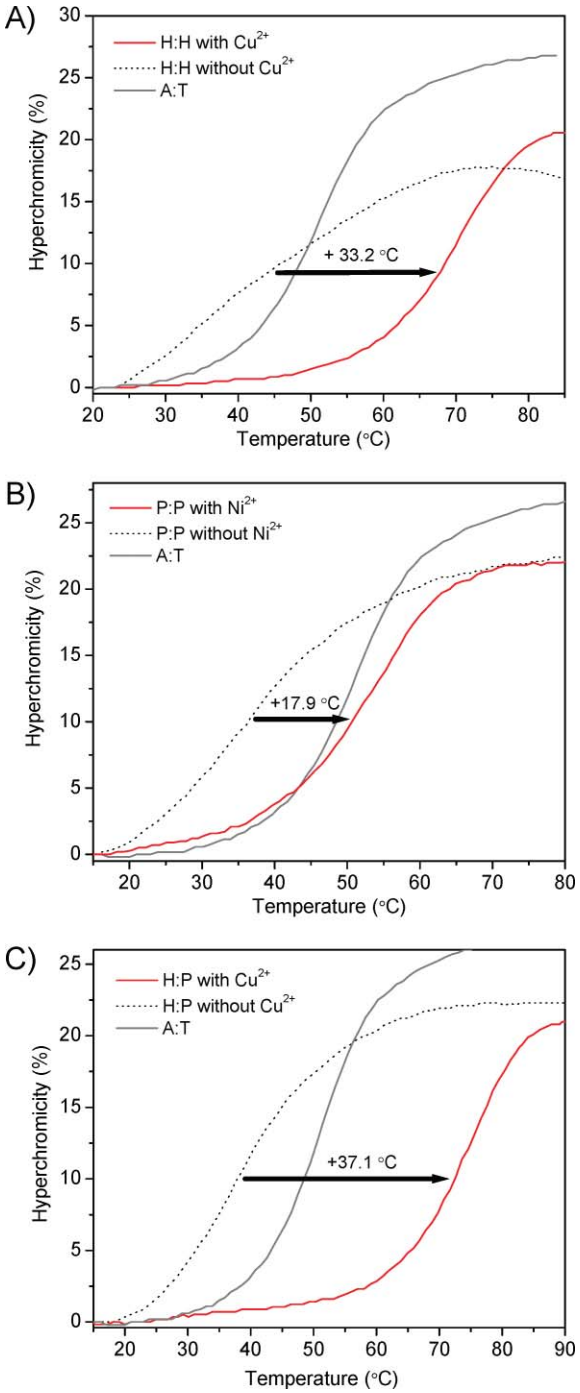

Fig. 2 Metal-dependent stabilities of duplexes containing hydroxypyridone (H) and pyridopurine (P) homo- and hetero-base pairs. A) Cu^{2+}-dependent UV-melting curves with the H:H base pair in GNA. B) Ni^{2+}-dependent UV-melting curves with the P:P base pair in GNA. C) Cu^{2+}-dependent UV-melting curves with the H:P base pair in GNA. All measurements were performed in 10 mM sodium phosphate buffer, 100 mM $NaNO_3$, pH = 7.0. Each sample contained 2 μM of each 15mer GNA strand (see Table 1 for sequences). $CuSO_4$ or $NiCl_2$ were added to a concentration of 4 μM.

at the same position (Table 1, entries 1 and 15). No significant stabilization can be observed with $Pd(NO_3)_2$, $AgNO_3$, $AuCl_3$, $Cd(NO_3)_2$ or $Ni(NO_3)_2$ (Table 1, entries 18–22); but $Co(NO_3)_2$

and $ZnCl_2$ stabilize the H:H base pair by 5.1 °C and 15.9 °C, respectively (Table 1, entries 16 and 17).

The copper(II)-induced stabilization of the hydroxypyridone base pair in GNA is surprisingly strong and significantly exceeds the reported stabilization for the analogous 2′-deoxynucleotide hydroxypyridone base pair in DNA for which for a stabilization of only 13.1 °C was reported in a 15mer duplex.[4] This indicates that the Cu^{2+}-mediated H:H base pair is particularly well accommodated in the GNA duplex compared to DNA.

Finally, we investigated the metal-mediated crosspairing of the hydroxypyridone and pyridopurine chelates (Table 1, entries 23–31). Overall, this hetero-base pair H:P behaves similarly to the hydroxypyridone homo-base pair H:H in its metal selectivities. In fact, the stabilization of H:P by Cu^{2+} exceeds the copper(II)-induced stabilization of H:H, affording a duplex with a T_M value of 74.4 °C. Thus, H:P is 23.9 °C more stable than an A:T base pair at the same position in the presence of Cu^{+2} ions. This higher stability can be rationalized by the higher hydrophobicity of P compared to H, whereas the steric problems within metal-coordinated P:P are absent in H:P.

Structure of the copper-mediated hydroxypyridone base pair in a GNA duplex

We recently determined the 1.3 Å crystal structure of an (*S*)-GNA duplex formed from the self-complementary strand 3′-CGHATHCG-2′ in which two copper(II)-hydroxypyridone base pairs served as handles to site-selectively introduce two heavy atoms per duplex for phasing the crystallographic data (Fig. 3).[8] Within the crystal, individual duplexes are coaxially stacked, thereby forming a continuous helix with a periodic pattern of copper(II) ions along the helix axis with Cu-Cu distances of 14.5 Å within a duplex and 23.7 Å between adjacent duplexes (Fig. 3A,B).

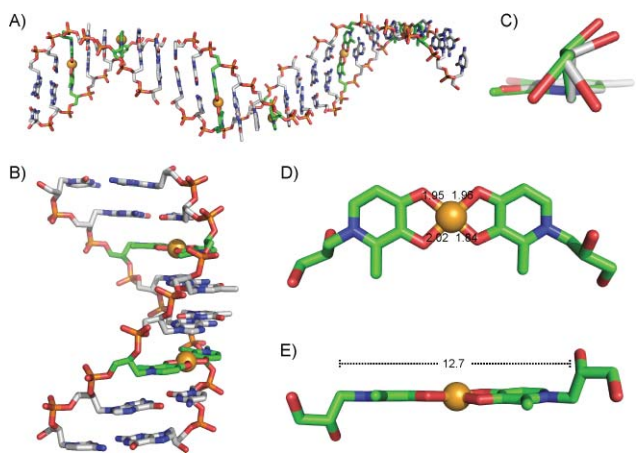

Fig. 3 Crystal structure of an 8mer GNA duplex with the self-complementary strand 3′-CGHATHCG-2′ in the presence of copper(II) (ref. 8). The metallo-base pairs are shown in green. A) Coaxially stacked 8mer duplexes form a continuous helix in the crystal with defined pattern of copper(II)-ions. B) An individual 8mer duplex. C) Superimposed hydroxypyridone and thymine nucleoside from the crystal structure indicating the differences in the conformation along $C_{2'}$–$C_{3'}$. D), E) Copper(II) coordination to hydroxypyridone nucleobases of opposite strands. Indicated are the coordinative bond length and the $C_{1'}$–$C_{1'}$ distance (in Å).

Within the metallo-base pair, a copper ion is coordinated by two hydroxypyridone nucleobases in an almost perfectly square planar fashion (Fig. 3D) with only a slight propeller twist of around 15° between the two chelating ligands. Coordinative bonds between the copper and oxygen ligands vary between 1.8 and 2.0 Å.

The high T_M values of duplexes containing the copper(II)-hydroxypyridone base pair and the crystal structure demonstrate that this metallo-base pair fits very well into the overall GNA duplex structure. This is surprising since the $C_{1'}$–$C_{1'}$ distance in this H:H base pair is 12.7 Å and thus exceeds the analogous $C_{1'}$–$C_{1'}$ distance of the natural A:T and G:C base pairs by around 2.0 Å (Fig. 3E). However, a closer look at the structure reveals that the hydroxypyridone nucleotide backbone compensates for this by rotating around the $C_{2'}$–$C_{3'}$ bond. In contrast to the natural nucleotides, in which the vicinal C–O bonds assume a *gauche* orientation, the glycolic C–O bonds of the hydroxypyridone nucleotides are oriented *anti* (Fig. 3C), which reduces the distances between the oxygens of paired nucleotides.

Conclusions

We here presented a full account of the incorporation of three metal-mediated base pairs into the simplified nucleic acid GNA by characterizing the pairing properties of pyridopurine and hydroxypyridone homo- and hetero-base pairs. Interestingly, it turns out that the properties of these metallo-base pairs are modulated in GNA compared to DNA with respect to base pairing stabilities and metal-selectivities. Most interestingly, the copper(II)-dependent stability of the GNA hydroxypyridone homo-base pair significantly exceeds the stability of this base pair in the context of duplex DNA and renders it, together with the hydroxypyridone-pyridopurine hetero-base pair, currently by far the most stable base pair in GNA. The application of such metallo-GNAs for the generation of duplexes with interesting electronic and magnetic properties is underway.

Experimental section

General procedures and reagents

NMR spectra were recorded on a Bruker DRX-500 (500 MHz), DRX-400 (400 MHz), DMX-360 (360 MHz), or DMX-300 (300 MHz) spectrometer. High-resolution mass spectra were obtained with a Micromass AutoSpec or Thermo LTQ-FT instrument using ES ionization. Infrared spectra were recorded either on a Perkin Elmer 1600 or Nicolet 510 series FTIR spectrometer. Solvents and reagents were used as supplied from Aldrich or Acros. Reactions were performed under an atmosphere of argon unless otherwise specified. Compound **3** was prepared as described previously.[7]

Compound 5

Compound **4** (1.3 g, 6.0 mmol) and NaH (60% in mineral oil, 50 mg, 1.3 mmol) were combined in DMF (12 mL) and stirred at room temperature under argon for one hour. A solution of **3** (2.1 g, 5.7 mmol) in DMF (12 mL) was added and the resulting mixture was heated to 110 °C overnight. The DMF was then evaporated, the residue taken up in ethyl acetate and concentrated to dryness. The crude product was purified by

column chromatography starting with EtOAc:Et_3N (100:1), then eluted with EtOAc:MeOH:Et_3N (40:3:0.01) to afford compound **5** as a light yellow foam (2.2 g, 65%). ^{1}H-NMR (500 MHz, $CDCl_3$) δ (ppm) 7.42 (d, J = 8.1 Hz, 2H), 7.37–7.20 (m, 13H), 6.83 (d, J = 8.2 Hz, 4H), 6.11 (d, J = 7.3 Hz, 1H), 5.08 (d, J = 11.3 Hz, 1H), 4.90 (d, J = 11.3 Hz, 1H), 4.14 (m, 2H), 3.79 (s, 6H), 3.52 (dd, J = 14.6, 9.7 Hz, 1H), 3.35 (dd, J = 9.2, 4.3 Hz, 1H), 3.10 (t, J = 8.4 Hz, 1H), 2.16 (s, 3H). ^{13}C-NMR (125 MHz, $CDCl_3$) δ (ppm) 173.0, 158.8, 145.9, 144.9, 142.2, 140.4, 137.8, 136.2, 136.0, 130.3, 129.1, 128.5, 128.4, 128.2, 128.1, 127.1, 116.5, 113.4, 86.5, 73.4, 68.9, 65.5, 58.6, 55.4, 12.9. IR (film) ν (cm^{-1}) = 3197, 3063, 2933, 2836, 1626, 1608, 1561, 1508, 1462, 1398, 1301, 1251, 1220, 1176, 1073, 1033, 980, 910, 827, 790, 753, 728, 701. HRMS calcd for $C_{37}H_{38}NO_6$ $(M + H)^+$ 592.2699, found $(M + H)^+$ 592.2727.

Compound 6

Compound **5** (1.5 g, 2.5 mmol) and Pd/C (10% on carbon, 750 mg) were combined in ethyl acetate (70 mL) and the resulting suspension was purged with argon, then H_2, and allowed to stir under a H_2 atmosphere for two hours. Filtration through Celite using EtOAc:Et_3N (100:1) afforded compound **6** as a tan foam (1.25 g, 98%) which was used without further purification. ^{1}H-NMR (500 MHz, $CDCl_3$) δ (ppm) 7.45 (d, J = 7.8 Hz, 2H), 7.37–7.15 (m, 8H), 6.86 (d, J = 8.5 Hz, 4H), 5.98 (br m, 1H), 5.42 (br s, 2H), 4.25 (d, J = 13.7 Hz, 1H), 4.03 (br s, 1H), 3.81 (s, 6H), 3.65 (m, 1H), 3.41 (m, 1H), 3.18 (m, 1H), 2.39 (s, 3H). ^{13}C-NMR (90 MHz, $CDCl_3$) δ (ppm) 168.7, 158.9, 145.7, 144.8, 138.5, 136.0, 135.8, 130.2, 129.4, 128.24, 128.18, 127.2, 113.5, 113.4, 110.8, 86.7, 69.2, 65.2, 58.0, 55.5, 12.4. IR (film) ν (cm^{-1}) = 3199, 3071, 2933, 2825, 1626, 1607, 1577, 1508, 1464, 1444, 1366, 1302, 1248, 1174, 1076, 1032, 909, 825, 791, 727, 702, 643, 584. HRMS calcd for $C_{30}H_{32}NO_6$ $(M + H)^+$ 502.2229, found $(M + H)^+$ 502.2248.

Compound 7

To an argon purged solution of compound **6** (415 mg, 0.83 mmol) and diphenylcarbamoyl chloride (230 mg, 0.99 mmol) in anhydrous pyridine (6.6 mL) was added diisopropylethylamine (175 μL, 0.99 mmol) and the solution stirred for one hour at room temperature under argon. The solution was poured into saturated aqueous $NaHCO_3$, extracted two times into dichloromethane, dried over Na_2SO_4, and finally concentrated by rotary evaporation. After coevaporation with toluene, the crude product was purified by column chromatography starting with EtOAc:Et_3N (100:1), then EtOAc:MeOH:Et_3N (50:1:0.01), and finally eluting with EtOAc:MeOH:Et_3N (40:3:0.01) to afford compound **7** as a light yellow foam (370 mg, 64%). ^{1}H-NMR (500 MHz, 373K, DMSO-d_6) δ (ppm) 7.50–7.20 (m, 20H), 6.89 (d, J = 8.8 Hz, 4H), 6.08 (d, J = 7.6 Hz, 1H), 4.13 (d, J = 11.4 Hz, 1H), 3.84 (m, 2H), 3.76 (s, 6H), 3.14 (dd, J = 9.3, 3.2 Hz, 1H), 3.00 (dd, J = 9.3, 6.1 Hz, 1H), 2.25 (s, 3H). ^{13}C-NMR (125 MHz, 373K, DMSO-d_6) δ (ppm) 169.2, 157.9, 150.9, 144.2, 142.3, 140.6, 140.4, 139.5, 135.3, 129.2, 128.3, 127.4, 127.2, 126.4, 126.1, 125.6, 114.5, 112.9, 85.5, 68.6, 64.9, 62.5, 55.2, 54.7, 12.0. IR (film) ν (cm^{-1}) = 3400 (br), 3059, 2928, 2833, 1742, 1644, 1608, 1598, 1512, 1494, 1352, 1306, 1250, 1218, 1200, 1176, 1151, 1053, 1025, 1002, 819, 757, 693. HRMS calcd for $C_{43}H_{41}N_2O_7$ $(M + H)^+$ 697.2908, found $(M + H)^+$ 697.2897.

Compound 1

To an argon purged solution of compound **7** (355 mg, 0.51 mmol) and diisopropylethylamine (510 μL, 2.9 mmol) in dichloromethane (8.5 mL) was added 2-cyanoethyl *N*,*N*′-diisopropylchlorophosphoramidite **8** (235 μL, 1.1 mmol) dropwise and the solution stirred for two hours at room temperature under argon. The solution was washed one time with saturated aqueous $NaHCO_3$, extracted into dichloromethane, dried over Na_2SO_4, and finally concentrated by rotary evaporation. The crude product was purified by column chromatography eluting with hexanes:acetone:Et_3N (1:1:0.01) to afford compound **1** as a white foam (395 mg, 86%). ^{31}P NMR (121 MHz, $CDCl_3$) δ (ppm) 150.6, 150.0. HRMS calcd for $C_{52}H_{58}N_4O_8P$ $(M + H)^+$ 897.3987, found $(M + H)^+$ 897.3973.

Compound 10

6-Chloropurine (**9**, 2.0 g, 12.9 mmol) and K_2CO_3 (230 mg, 1.7 mmol) were combined in DMF (20 mL). A solution of epoxide **3** (4.7 g, 12.5 mmol) in DMF (20 mL) was added and the resulting mixture was heated to 90 °C overnight. The DMF was then evaporated, the residue taken up in ethyl acetate and concentrated to dryness. The crude product was purified by column chromatography starting with hexanes:EtOAc:Et_3N (1:1:0.01), then eluting with hexanes:EtOAc:Et_3N (1:2:0.01) to afford compound **10** as a white foam (2.5 g, 38%). ^{1}H-NMR (360 MHz, $CDCl_3$) δ (ppm) 8.69 (s, 1H), 8.16 (s, 1H), 7.40 (m, 2H), 7.34–7.20 (m, 7H), 6.83 (m, 4H), 4.51 (dd, J= 14.3, 3.0 Hz, 1H), 4.35 (dd, J= 14.3, 7.1 Hz, 1H), 4.22 (m, 1H), 3.81 (s, 6H), 3.48 (b, 1H), 3.20 (d, J= 5.6 Hz, 2H). ^{13}C-NMR (90 MHz, $CDCl_3$) δ (ppm) 159.0, 152.2, 152.0, 151.3, 146.8, 144.6, 135.73, 135.71, 131.7, 130.2, 128.31, 128.25, 127.4, 87.0, 69.5, 64.8, 55.6, 48.0. IR (film) ν (cm^{-1}) = 3317, 2933, 2835, 1666, 1602, 1592, 1562, 1508, 1464, 1445, 1405, 1336, 1302, 1253, 1179, 1076, 1032, 948, 909, 830, 727, 702, 643. HRMS calcd for $C_{29}H_{27}N_4O_4Cl$ $(M + H)^+$ 531.1799, found $(M + H)^+$ 531.1805.

Compound 11

Compound **10** (2.6 g, 4.9 mmol) was dissolved in dichloromethane (22 mL) under argon and TBSCl (1.7 g, 11.3 mmol), imidazole (3.0 g, 44.1 mmol), and catalytic DMAP added to the solution. This was allowed to stir overnight at room temperature and then concentrated by rotary evaporation the next morning. The crude product was purified by column chromatography starting with hexanes:EtOAc:Et_3N (6:1:0.01), then eluting with hexanes:EtOAc:Et_3N (4:1:0.01) to afford compound **11** as a white foam (2.7 g, 86%). ^{1}H-NMR (360 MHz, $CDCl_3$) δ (ppm) 8.73 (s, 1H), 8.12 (s, 1H), 7.43 (d, J = 7.3 Hz, 2H), 7.35–7.19 (m, 7H), 6.82 (m, 4H), 4.56 (dd, J = 14.1, 3.9 Hz, 1H), 4.44 (dd, J = 14.0, 6.6 Hz, 1H), 4.15 (m, 1H), 3.80 (s, 6H), 3.14 (dd, J = 9.8, 4.2 Hz, 1H), 3.00 (dd, J = 9.6, 7.1 Hz, 1H), 0.79 (s, 9H), -0.16 (s, 3H), -0.33 (s, 3H). ^{13}C-NMR (75 MHz, $CDCl_3$) δ (ppm) 158.76, 158.74, 152.3, 151.9, 150.9, 146.5, 144.6, 135.8, 135.7, 131.4, 130.0, 128.2, 128.0, 127.1, 113.3, 86.6, 69.8, 64.7, 55.3, 48.0, 25.8, 17.9, -4.8, -5.4. IR (film) ν (cm^{-1}) = 2954, 2927, 2858, 1608, 1590, 1560, 1508, 1464, 1442, 1403, 1333, 1302, 1246, 1176, 1080, 1036, 997, 940, 831, 779, 726, 700. HRMS calcd for $C_{35}H_{41}N_4O_4SiCl$ $(M + H)^+$ 645.2664, found $(M + H)^+$ 645.2683.

Compound 13

To an argon purged solution of compound **11** (2.7 g, 4.2 mmol) and $PdCl_2(PPh_3)_2$ (265 mg, 0.4 mmol) in anhydrous THF (85 mL) was added 2-pyridylzinc bromide (**12**, 0.5 M in THF, 13.5 mL) and the solution heated to 65 °C for two hours. After cooling to room temperature, the solution was washed with saturated aqueous $NaHCO_3$, extracted into dichloromethane, dried over Na_2SO_4, and concentrated by rotary evaporation. The crude product was purified by column chromatography over basic alumina starting with hexanes:EtOAc:Et_3N (3:1:0.01), then using hexanes:EtOAc:Et_3N (1:1:0.01), and finally eluting with EtOAc:Et_3N (100:1) to afford compound **13** as a tan foam (2.3 g, 81%). ^{1}H-NMR (400 MHz, $CDCl_3$) δ (ppm) 9.12 (s, 1H), 8.97 (m, 1H), 8.86 (d, J = 8.0 Hz, 1H), 8.23 (s, 1H), 7.93 (td, J = 7.7, 1.6 Hz, 1H), 7.45 (m, 3H), 7.31 (m, 6H), 7.21 (t, J = 7.2 Hz, 1H), 6.82 (dd, J = 8.9, 2.5 Hz, 4H), 4.60 (dd, J = 14.1, 3.7 Hz, 1H), 4.50 (dd, J = 14.1, 6.7 Hz, 1H), 4.21 (m, 1H), 3.77 (s, 6H), 3.16 (dd, J = 9.8, 4.2 Hz, 1H), 3.07 (dd, J = 9.8, 7.0 Hz, 1H), 0.79 (s, 9H), -0.16 (s, 3H), -0.34 (s, 3H). ^{13}C-NMR (125 MHz, $CDCl_3$) δ (ppm) 158.73, 158.71, 154.0, 153.7, 153.3, 152.6, 150.6, 146.8, 144.7, 136.8, 136.0, 135.9, 130.1, 128.2, 128.0, 127.0, 126.0, 124.9, 113.3, 86.6, 69.9, 64.9, 55.3, 47.7, 25.8, 17.9, -4.8, -5.3. IR (film) ν (cm^{-1}) = 3499, 2956, 2929, 2853, 1612, 1581, 1510, 1463, 1441, 1384, 1325, 1301, 1251, 1174, 1116, 1068, 1030, 988, 929, 825, 773, 720, 692, 635, 570, 531. HRMS calcd for $C_{40}H_{45}N_5O_4Si$ $(M + H)^+$ 688.3319, found $(M + H)^+$ 688.3314.

Compound 14

To an argon purged solution of compound **13** (1.25 g, 1.8 mmol) in anhydrous THF (38 mL) was added TBAF (1 M in THF, 4 mL) and the solution stirred for 30 minutes at room temperature. The solution was washed with water, extracted into ethyl acetate, dried over Na_2SO_4, and concentrated by rotary evaporation. The crude product was purified by column chromatography over basic alumina starting with EtOAc:Et_3N (100:1), then eluting with EtOAc:MeOH:Et_3N (40:3:0.01) to afford compound **14** as a tan foam (840 mg, 81%). ^{1}H-NMR (400 MHz, $CDCl_3$) δ (ppm) 9.04 (s, 1H), 8.95 (m, 1H), 8.82 (m, 1H), 8.22 (s, 1H), 7.93 (td, J = 7.8, 1.8 Hz, 1H), 7.46–7.38 (m, 3H), 7.31–7.25 (m, 6H), 7.21 (m, 1H), 6.81 (m, 4H), 4.54 (dd, J = 14.4, 2.8 Hz, 1H), 4.39 (dd, J = 14.3, 7.0 Hz, 1H), 4.22 (m, 1H), 3.76 (s, 6H), 3.24 (dd, J = 9.8, 5.9 Hz, 1H), 3.17 (dd, J = 9.7, 5.6 Hz, 1H). ^{13}C-NMR (100 MHz, $CDCl_3$) δ (ppm) 158.8, 153.8, 153.5, 153.4, 152.3, 150.5, 146.9, 144.6, 136.9, 135.7, 135.6, 130.0, 128.08, 128.07, 127.1, 125.9, 125.0, 113.4, 86.7, 69.6, 64.7, 55.3, 47.9, 25.8. IR (film) ν (cm^{-1}) = 3369, 3060, 2953, 2931, 2833, 1612, 1582, 1509, 1462, 1444, 1328, 1302, 1252, 1209, 1175, 1152, 1069, 1031, 905, 828, 726, 697, 637, 577. HRMS calcd for $C_{34}H_{31}N_5O_4$ $(M + H)^+$ 574.2454, found $(M + H)^+$ 574.2449.

Compound 2

To an argon purged solution of compound **14** (705 mg, 1.2 mmol) and diisopropylethylamine (1.0 mL, 5.9 mmol) in dichloromethane (20 mL) was added 2-cyanoethyl *N*,*N*′-diisopropylchlorophosphoramidite (560 μL, 2.5 mmol) dropwise and the solution stirred for two hours at room temperature under argon. After the addition of dichloromethane, the solution was washed one time with saturated aqueous $NaHCO_3$, dried over Na_2SO_4, and finally concentrated by rotary evaporation. The crude product was purified by column chromatography over basic alumina starting with hexanes:EtOAc:Et_3N (1:1:0.01), then using hexanes:EtOAc:Et_3N (1:2:0.01), and finally eluting with EtOAc:Et_3N (100:1) to afford compound **2** as a light yellow foam (620 mg, 65%). ^{31}P-NMR (121 MHz, $CDCl_3$) δ (ppm) 150.5, 150.0. HRMS calcd for $C_{43}H_{48}N_7O_5P$ $(M + H)^+$ 774.3533, found $(M + H)^+$ 774.3527.

GNA oligonucleotide synthesis and purification

GNA oligonucleotides were prepared on an ABI 394 DNA/RNA synthesizer on a one micromole scale. GNA phosphoramidites (A, T, G, C, **1**, **2**) were used at a concentration of 100 mM with a standard protocol for 2-cyanoethyl phosphoramidites, except that the coupling was extended to 3 minutes (A, T, G, C), or 8 minutes (**1**, **2**). After the trityl-on synthesis, the resin was incubated with concentrated aqueous ammonia at 55–60 °C for 12 hours and then evaporated. The tritylated oligonucleotides were purified by C_{18} reversed-phase HPLC (Varian Dynamax 250 × 10 mm, Microsorb 300–10, C_{18}) with aqueous triethylammonium acetate (50 mM TEAA) and acetonitrile as the eluent. The oligonucleotides were then detritylated with 80% acetic acid for 20 min and precipitated with *i*PrOH after addition of 3 M sodium acetate. All oligonucleotides were finally purified at 55–60 °C using a Waters XTerra column (MS C18, 4.6 × 50 mm, 2.5 μm) with aqueous TEAA (50 mM) and acetonitrile as the eluent. All identities were confirmed by MALDI-TOF MS and purities confirmed by HPLC and MALDI-TOF analysis. Extinction coefficients for GNA (strands shown in 3′→2′ direction) were calculated from deoxynucleotide increments and yielded the following values for ε_{260} ($M^{-1}cm^{-1}$): AAT ATT ATT ATT TTA (153630), TAA AAT AAT AAT ATT (171720), AAT ATT AHT ATT TTA (150606), TAA AAT AHT AAT ATT (162666), AAT ATT APT ATT TTA (159660), TAA AAT APT AAT ATT (171720), TAA AAT ATT AAT ATT (165690).

Metal dependent thermal stability of (*S*)-GNA duplexes monitored by UV spectroscopy

The melting studies were carried out in 1 cm path length quartz cells (200 μL sample solution covered by mineral oil) on a Beckman DU800 spectrophotometer equipped with a thermoprogrammer. Stock solutions of GNA strands (10 μM) were prepared in a 10 mM sodium phosphate buffer, pH 7.0, containing 100 mM $NaNO_3$ and subsequently treated with Chelex resin overnight. The stock oligos were then combined with the respective metals (2 equivalents) and diluted to a final duplex concentration of 2 μM. Melting temperatures were calculated using a nonlinear fit to the heating curves. Experiments were performed at least in duplicate and the averages taken.

Acknowledgements

We thank the Philipps-University Marburg for financial support.

References

1 For DNA nanotechnology, see: N. C. Seeman, *Chem. Biol.*, 2003, **10**, 1151–1159; N. C. Seeman, *Mol. Biotechnol.*, 2007, **37**, 246–257.
2 For modified nucleic acids, see: S. M. Freier and K.-H. Altmann, *Nucleic Acids Res.*, 1997, **25**, 4429–4443; A. Eschenmoser, *Science*,

1999, **284**, 2118–2124; E. T. Kool, *Acc. Chem. Res.*, 2002, **35**, 936–943; C. J. Leumann, *Bioorg. Med. Chem.*, 2002, **10**, 841–854; A. A. Henry and F. E. Romesberg, *Curr. Opin. Chem. Biol.*, 2003, **7**, 727–733; S. A. Benner, *Acc. Chem. Res.*, 2004, **37**, 784–797.

3 E. Meggers, P. L. Holland, W. B. Tolman, F. E. Romesberg and P. G. Schultz, *J. Am. Chem. Soc.*, 2000, **122**, 10714–10715; S. Atwell, E. Meggers, G. Spraggon and P. G. Schultz, *J. Am. Chem. Soc.*, 2001, **123**, 12364–12367; N. Zimmermann, E. Meggers and P. G. Schultz, *J. Am. Chem. Soc.*, 2002, **124**, 13684–13685; N. Zimmermann, E. Meggers and P. G. Schultz, *Bioorg. Chem.*, 2004, **32**, 13–25; J. Mueller, D. Boehme, P. Lax, M. M. Cerda and M. Roitzsch, *Chem. Eur. J.*, 2005, **11**, 6246–6253; G. H. Clever, K. Polborn and T. Carell, *Ang. Chem., Int. Ed.*, 2005, **44**, 7204–7208; C. Switzer and D. Shin, *Chem. Commun.*, 2005, 1342–1344; Y. Miyake, H. Togashi, M. Tashiro, H. Yamaguchi, S. Oda, M. Kudo, Y. Tanaka, Y. Kondo, R. Sawa, T. Fujimoto, T. Machinami and A. Ono, *J. Am. Chem. Soc.*, 2006, **128**, 2172–2173; G. H. Clever, Y. Soeltl, H. Burks, W. Spahl and T. Carell, *Chem. Eur. J.*, 2006, **12**, 8708–8718; K. Tanaka, G. H. Clever, Y. Takezawa, Y. Yamada, C. Kaul, M. Shionoya and T. Carell, *Nat. Nanotechnol.*, 2006, **1**, 190–194; G. H. Clever and T. Carell, *Angew. Chem., Int. Ed.*, 2007, **46**, 250–253; D. Shin and C. Switzer, *Chem. Commun.*, 2007, **42**, 4401–4403; D. Boehme, N. Duepre, D. A. Megger and J. Mueller, *Inorg. Chem.*, 2007, **46**, 10114–10119; F.-A. Polonius and J. Mueller, *Angew. Chem., Int. Ed.*, 2007, **46**, 5602–5604; B. D. Heuberger, D. Shin and C. Switzer, *Org. Lett.*, 2008, **10**, 1091–1094.

4 K. Tanaka, A. Tengeiji, T. Kato, N. Toyama, M. Shiro and M. Shionoya, *J. Am. Chem. Soc.*, 2002, **124**, 12494–12498.

5 C. Switzer, S. Sinha, P. H. Kim and B. D. Heuberger, *Angew. Chem., Int. Ed.*, 2005, **44**, 1529–1532.

6 For reviews on metallo-base pairing, see: H.-A. Wagenknecht, *Angew. Chem., Int. Ed.*, 2003, **42**, 3204–3206; M. Shionoya and K. Tanaka, *Curr. Opin. Chem. Biol.*, 2004, **8**, 592–597; G. H. Clever, C. Kaul and T. Carell, *Angew. Chem., Int. Ed.*, 2007, **46**, 6226–6236.

7 L. Zhang, A. Peritz and E. Meggers, *J. Am. Chem. Soc.*, 2005, **127**, 4174–4175; L. Zhang and E. Meggers, *Synthesis*, 2006, 645–653; M. K. Schlegel, A. E. Peritz, K. Kittigowittana, L. Zhang and E. Meggers, *ChemBioChem*, 2007, **8**, 927–932.

8 M. K. Schlegel, L.-O. Essen and E. Meggers, *J. Am. Chem. Soc.*, 2008, **130**, 8158–8159.

9 Y.-W. Yang, S. Zhang, E. O. McCullum and J. C. Chaput, *J. Mol. Evol.*, 2007, **65**, 289–295; C.-H. Tsai, J. Y. Chen and J. W. Szostak, *Proc. Natl. Acad. Sci. U. S. A.*, 2007, **104**, 14598–14603; A. T. Horhota, J. W. Szostak and L. W. McLaughlin, *Org. Lett.*, 2006, **8**, 5345–5347; R. S. Zhang, E. O. McCullum and J. C. Chaput, *J. Am. Chem. Soc.*, 2008, **130**, 5846–5847.

10 For metallo-base pairing in PNA, see: D.-L. Popescu, T. J. Parolin and C. Achim, *J. Am. Chem. Soc.*, 2003, **125**, 6354–6355; R. M. Watson, Y. A. Skorik, G. K. Patra and C. Achim, *J. Am. Chem. Soc.*, 2005, **127**, 14628–14639; B. P. Gilmartin, K. Ohr, R. L. McLaughlin, R. Koerner and M. E. Williams, *J. Am. Chem. Soc.*, 2005, **127**, 9546–9555.

11 A. Gold and R. Sangaiah, *Nucleosides Nucleotides*, 1990, **9**, 907–912.

12 M. Hoffer, *Chem. Ber.*, 1960, **93**, 2777–2781.

13 Z. Kazimierczuk, H. B. Cottam, G. R. Revankar and R. K. Robins, *J. Am. Chem. Soc.*, 1984, **106**, 6379–6382.

